IEEE Access
Multidisciplinary ⋮ Rapid Review ⋮ Open Access Journal

Received 13 April 2023, accepted 31 May 2023, date of publication 12 June 2023, date of current version 28 June 2023.

Digital Object Identifier 10.1109/ACCESS.2023.3285281

RESEARCH ARTICLE

A Study on Sound Radiation Characteristics of Slim Speaker System

JOON-YEON PARK AND JE-HEON HAN, (Member, IEEE)
Department of Mechanical Engineering, Tech University of Korea, Siheung-si, Geonggi-do 15073, South Korea

Corresponding author: Je-Heon Han (jeep2000@tukorea.ac.kr)

This work was supported in part by the National Research Foundation of Korea (NRF) funded by the Ministry of Education, Science and Technology under Grant NRF-2017R1A6A1A03015562 and Grant NRF-2021R1F1A1056483; and in part by the GRRC Program of Gyeonggi Province through the Multi-Material Machining Innovative Technology Research Center under Grant GRRC TUKorea2020-B03.

ABSTRACT For ultra-thin TVs, slim speaker enclosures are usually used to reduce the thickness. These slim speaker systems can suffer from acoustic problems such as poor radiated sound performance in a specific frequency range. This paper studies the sound radiation performance improvement of the slim speaker system. First, it experimentally confirms the poor frequency response at the specific frequency of the speaker system. Then, it is investigated why the speaker frequency response is poor at the frequency through the numerical method. It is found that the radiated sound pressure decreases due to the destructive interference caused by the 180-degree phase difference between the incidence wave and the reflected wave at the corresponding frequency. To improve sound radiation performance, three types of noise control methods are suggested: (1) installing a sound-absorbing material, (2) installing a membrane on the reflective surface in the enclosure, and (3) providing a slit at the top of the enclosure. The proposed method is verified through experiments.

INDEX TERMS FEA, slim speaker, sound radiation, waveguide.

I. INTRODUCTION

Customer demand and technological development lead to a thickness decrease in electronic devices. Especially for the TV, its thickness dramatically has decreased with the development of display technology [1]. In the case of the CRT (Cathode Ray Tube), it was very thick due to the presence of electron guns. Therefore, the thickness of the TV speakers was not an issue then. However, as the thickness of the display becomes thinner and thinner, the size of its speaker has come to dominate the total thickness of the TV [2]. In addition to the TV, the size of the speaker is considered an essential factor in determining the thickness of mobile devices such as laptops, cellphones, and tablets [3]. For this reason, thin enclosures were designed for slim TVs to radiate sound efficiently [4], and slim speaker systems with waveguides have been actively studied [5], [6], [7], [8].

Generally, the speaker is installed on the enclosure to achieve monopole-like radiation since acoustic cancellation can be prevented [9]. A closed enclosure is usually applied to the speaker, and a passive radiator also is used to improve the low-frequency response. In addition, various types of enclosures, such as a base-reflex enclosure using a duct [10] or a port [11] are used depending on their purposes.

However, by mounting the speaker on the enclosure, resonant standing wave fields can be generated, and a peak or dip in the frequency domain is obtained corresponding to the size of the enclosure. To prevent acoustic resonance, a sound-absorbing material is applied to the enclosure [8]. Various studies have been conducted to reduce the acoustic resonance effect of the speaker system with the enclosure. Jiang et al. installed a screen to remove peaks and dips caused by the influence of standing waves in a speaker enclosure [12]. Lee et al. improved the frequency response by changing the enclosure structure of the TV [13], and Fahy et al. showed that the acoustic resonance mode generated in the enclosure could be controlled by using the Helmholtz resonator [14]. In addition, Li et al. controlled the resonance mode in the enclosure more effectively by applying

The associate editor coordinating the review of this manuscript and approving it for publication was Jingang Jiang.

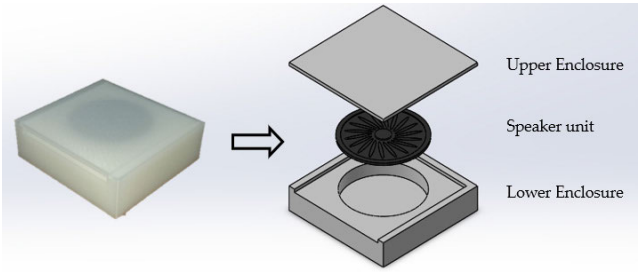

FIGURE 1. Slim speaker assembly.

the Helmholtz resonator array [15], and Park et al. reduced the low-frequency noise in the enclosure using the Helmholtz array [16].

Although it is necessary to use a slim speaker to make the TV thinner, many problems, such as non-uniform frequency response, relatively low sound radiation, and inefficient response in the low-frequency range, can occur [17]. Therefore, an alternative system other than the existing slim speaker was also proposed. To overcome the limited space inside the TV and increase the sound radiation performance, Demiel made an additional structure at the bottom of the TV to install a thick speaker [17]. Recently, according to the development of the display device, SOD (Sound on Display), a type of speaker in which the OLED panel acts as a diaphragm by attaching an exciter to the back of the panel, has been used [13].

This paper analyzes the acoustic radiation characteristics obtained from a speaker emitting sound laterally through the waveguide. This type of speaker system [18] has a problem in that radiated sound pressure decreases in a specific frequency region. Therefore, by building a speaker model, it is shown that it has poor sound radiation performance at specific frequencies experimentally and numerically. It is confirmed that the FE analysis response is consistent with the experimental results. Then, based on the correlated FE model, the poor frequency response of the speaker system at the specific frequency is investigated. Then, some methods are proposed to improve the speaker system's frequency response and validated through the experimental results.

II. REPRODUCING PROBLEM THROUGH EXPERIMENT

To experimentally reproduce the poor sound radiation problem of the slim speaker system, the authors fabricate a speaker assembly, as shown in Fig.1, and the frequency response is measured. For the speaker, a commercial speaker with a diameter of 50 mm, RMS power of 1 W, and impedance of 8 Ω is used. Its enclosure is made of PLA-i21 material using a 3D printer.

For the acoustic data acquisition, a Siemens SCADAS Mobile system and a 1/4 inch PCB microphone 130F20 are used to measure the radiated sound pressure in an anechoic chamber, as shown in Fig. 2. White random noise with frequencies up to 5 kHz is generated by the Simcenter Testlab Software. The microphone is installed horizontally

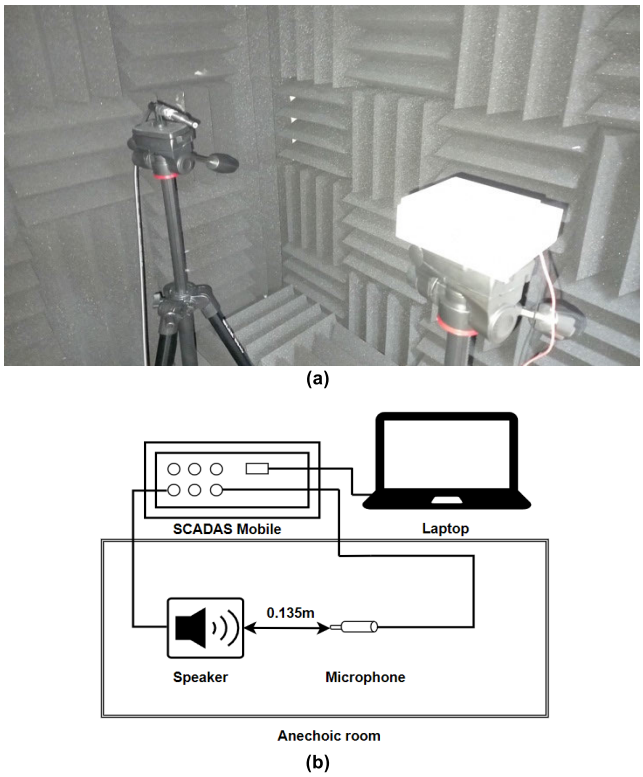

FIGURE 2. Experimental setup: (a) Radiated noise measurement setup of slim speaker system and (b) Schematic experimental setup.

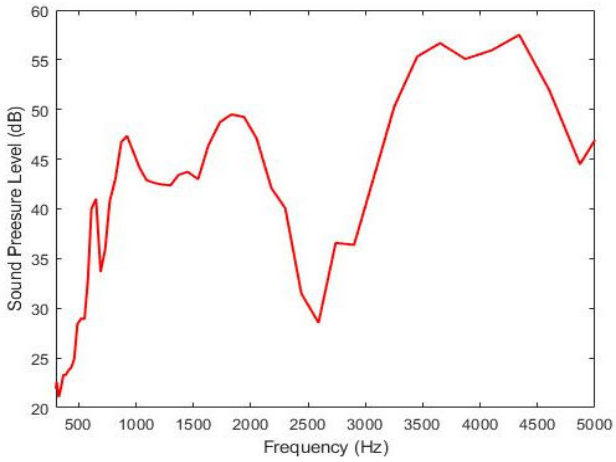

FIGURE 3. Measured sound pressure level.

0.135 m away from the sound path where the sound is radiated.

Fig. 3 shows the measured sound pressure level in the 1/12 octave band. It can be observed that there is a dip in the frequency range from 2400 Hz to 2700 Hz, and the frequency response is significantly poor in this range.

III. PROBLEM INVESTIGATION THROUGH NUMERICAL ANALYSIS

In this chapter, the main reasons for the poor sound radiation in the specific frequency range are investigated by using a

FEM software package, COMSOL Multiphysics. To focus on the investigation of the geometric effect of the speaker enclosure, a simplified model is used for the numerical analysis.

A. ACOUSTIC ANALYSIS WITH POINT SOURCE

In order to reduce the analysis time and efficiently identify the effect of the enclosure shape on the frequency response of the slim speaker system, the analysis model is simplified with the following assumptions.

1. Consider the speaker as a monopole sound source.
2. Assume that the enclosure is a rigid body.
3. Neglect structure-acoustic coupling effect due to the structural vibration of the enclosure.

The simplified model used in the numerical analysis is shown in Fig. 4, and the frequency response is obtained as shown in Fig. 5. It can be observed that a dip occurs at about 2500 Hz, similar to the test result.

To better understand the cause of the dip, additional numerical analysis is performed by varying the sound source's location and the enclosure's length. Fig. 6(a) is the result of the analysis by moving the noise source, and Fig. 6(b) is the analysis performed while adjusting the dimensions of the enclosure. Table 1 shows the dip frequencies at which the sound radiation is poor for each condition and the quarter-wavelength corresponding to the dip frequencies. By changing the source position and the enclosure length, the causes of poor sound radiation are identified. From the numerical analysis results, it can be confirmed that the 1/4 wavelengths corresponding to the dip frequencies match well the distance between the sound source and the enclosure wall (i.e., L_{gap} – source position ≈ corresponding 1/4 wavelength in Table 1).

In addition to the dip frequency, the first peak frequency of the calculated sound pressure level is also investigated. In Table 2, the frequency corresponding to the 1/4 wavelength of the acoustic passage length is compared with the first peak of the calculated sound pressure level. It can be observed that they have slightly different values. An end correction is applied to modify the length L to compensate for this discrepancy. The formula for correcting the length L is as follows [19], [20].

$$f_{res} = \frac{c}{4L_c} \tag{1}$$

$$L_c \cong L + 0.31D \tag{2}$$

where f_{res} is the theoretical quarter wavelength resonance frequency, c is the speed of sound in air, L_c is the modified, equivalent length, and D is the diameter of the acoustic path. The above equation is a correction equation assuming that the cross-section is circular. In order to check whether the error is due to the correction effect, an open-closed-end pipe is generated, as shown in Fig. 7, and the numerical analysis is conducted by changing the length and diameter of the enclosure with keeping the distance between the right wall and the sound source location at 35 mm.

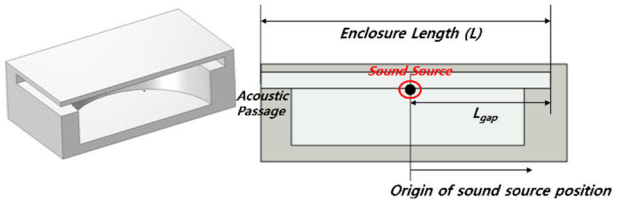

FIGURE 4. Shape of simplified slim speaker.

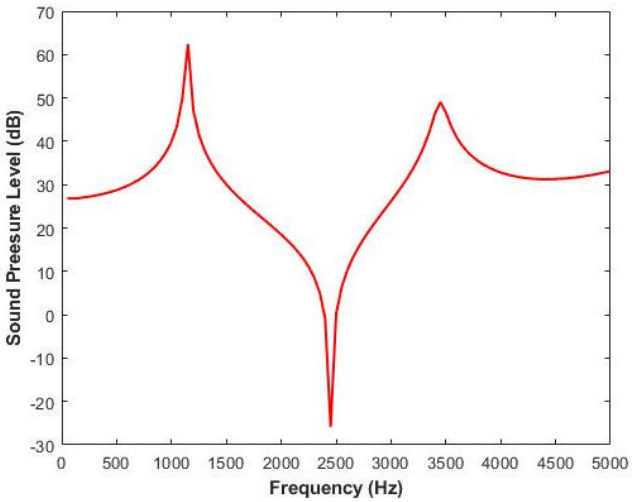

FIGURE 5. Calculated sound pressure level.

TABLE 1. Dip frequencies according to source location and enclosure length (L_{gap}).

Source position [mm]	Length (L_{gap}) [mm]	Dip frequency [Hz]	1/4 wavelength [mm]
-3		2250	38.1
0	35	2450	35.0
3		2700	31.8
	32	2700	31.8
0	35	2450	35.0
	38	2250	38.1

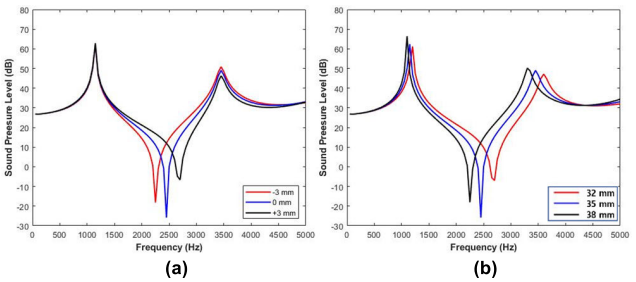

FIGURE 6. Sound pressure level of simplified slim speaker generated by monopole source (a) according to sound source location and (b) distance between sound source and enclosure wall.

Table 3 shows the modified quarter-wavelength resonance frequencies using Eqs. (1), (2) and the first peak frequencies obtained from the numerical analysis. It shows that they

TABLE 2. Quarter wavelength resonance frequency and 1st peak frequency of calculated sound pressure level of simplified slim speaker.

Enclosure length, L [mm]	1/4 wavelength frequency corresponding to L, f_{res} [Hz]	1st peak frequency of calculated SPL [Hz]
68	1136	1200
71	1106	1150
74	1078	1100

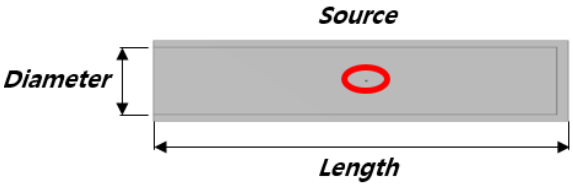

FIGURE 7. Simplified model to check end correction.

TABLE 3. Modified quarter wavelength resonance frequency and 1st peak frequency of calculated sound pressure level of open-closed-end pipe.

Enclosure length, L [mm]	Diameter, D [mm]	1/4 wavelength frequency corresponding to L_c [Hz]	1st peak frequency of calculated SPL [Hz]
68		1155	1150
71	20	1110	1106
74		1069	1066
	12	1148	1144
71	20	1110	1106
	28	1076	1072

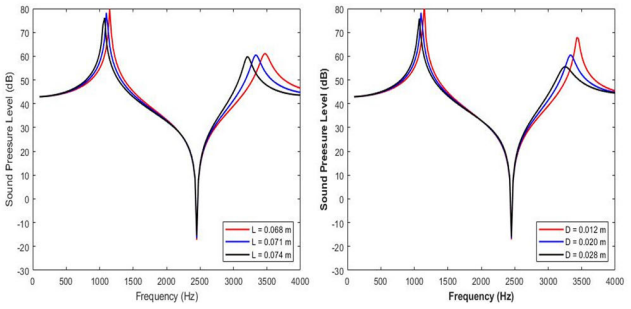

FIGURE 8. Sound pressure level of simplified slim speaker generated by monopole source (a) according to sound source location and (b) distance between sound source and enclosure wall.

match well when the end correction is considered. In addition, as shown in Fig. 8, since the distance between the wall and the sound source is kept constant, it can be observed that the dip frequency remains unchanged. Therefore, it can be confirmed that the first peak frequency is generated since the acoustic passage acts as a quarter-wavelength resonator.

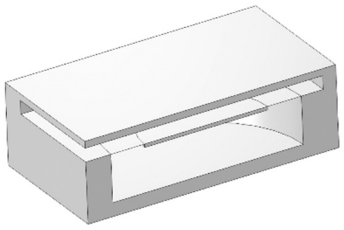

FIGURE 9. Shape of simplified slim speaker systemwith diaphragm source.

TABLE 4. Dip frequencies according to source location and enclosure length (L_{gap}) for structural-acoustic coupling analysis.

Source center position [mm]	Length (L_{gap}) [mm]	Dip frequency [Hz]	1/4 wavelength corresponding to dip frequency [mm]
-3		2250	38.1
0	35	2450	35.0
3		2700	31.8
	32	2700	31.8
0	35	2450	35.0
	38	2250	38.1

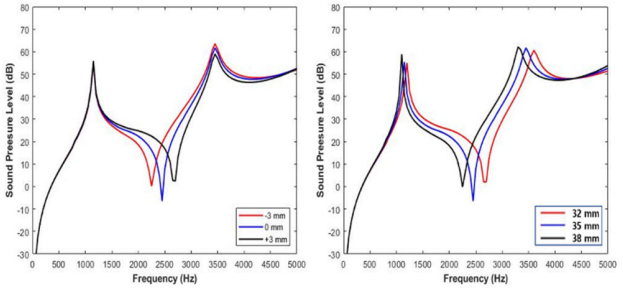

FIGURE 10. Sound pressure level of simplified slim speaker generated by circular diaphragm source (a) according to sound source location and (b) distance between sound source and enclosure wall.

B. STRUCTURE-ACOUSTIC COUPLING ANALYSIS WITH CIRCULAR DIAPHRAGM SOUND SOURCE

In this chapter, as shown in Fig. 9, numerical analysis is performed using a finite-sized circular diaphragm as a sound source rather than a point source. Structural-acoustic coupling analysis is applied to consider the effect of structural resonance, such as the resonance mode of a diaphragm or enclosure. A uniformly distributed normal force is applied on the lower surface of the diaphragm at all frequencies. The changes in sound pressure are investigated by moving the sound source's location and adjusting the enclosure's length to understand the frequency response of the slim speaker system more systematically.

Table 4 summarizes the dip frequency and the corresponding quarter wavelength for each condition. The detailed frequency response is shown in Fig. 10. Fig. 10(a) shows the result of the analysis by moving the sound source, and

Fig. 10(b) shows the analysis result performed by adjusting the dimensions of the enclosure (L_{gap}). Similar to the results in Section III-A, the dip frequency matches well with the quarter wavelength frequency corresponding to the distance between the sound source and the rigid wall. As shown in Fig. 10(a), even if the sound source is moved, the first peak frequency does not change because the enclosure size does not change, but the dip frequency varies since the distance from the sound source to the right wall changes. Fig. 10(b) shows that there is a change in the first peak frequency due to a change in the corresponding quarter-wave frequency (i.e., a change in the size of the enclosure) and also a change in the dip frequency because the distance from the sound source to the right wall also changes. Through this observation, it can be seen that the leading cause of peaks and dips is the shape of the enclosure rather than the influence of the sound source, such as the resonance modes of the diaphragm.

These analyses show that the first peak of the radiated sound pressure level is correlated with the longitudinal shape inside the enclosure and corresponds to the quarter wavelength resonance by considering the end correction effect. In addition, the dip frequency is caused by the 180-degree phase difference between the propagated wave component directly radiated through the acoustic passage and the reflected wave component corresponding to a quarter wavelength distance (i.e., 1/2 wavelength in the round trip), and it is estimated that the radiation performance becomes abysmal [21].

IV. ENCLOSURE STRUCTURE IMPROVEMENT CONSIDERING ACOUSTIC CHARACTERISTICS

In this chapter, the poor sound radiation performance at the dip frequency is improved by modifying the structure of the enclosure. To achieve this goal, four methods are suggested.

A. APPLYING SOUND-ABSORBING MATERIAL

In the last chapter, it was confirmed that the dip occurs due to the influence of the reflected wave from the inner wall of the enclosure. Therefore, it can be assumed that the dip can be suppressed by reducing the reflected wave. For this purpose, sound-absorbing material is applied to the wall, and numerical analysis is performed, as shown in Fig. 11. One of the analysis conditions in Section III-B is used. (i.e., the source center is 0 mm, and L_{gap} is 35 mm.) Fig. 12 shows the frequency response according to the absorption coefficient. It can be observed that the dip gradually disappears as the reflected wave is reduced by increasing the sound absorption coefficient, and the first peak also disappears as the quarter wavelength resonance decreases. For an actual sound-absorbing material, the sound absorption coefficient changes according to the frequency. In the case of the slim speaker system, getting enough space to install the sound-absorbing material is not easy to achieve a sufficient sound absorption coefficient. For this reason, another method is proposed to reduce the effect of reflected waves.

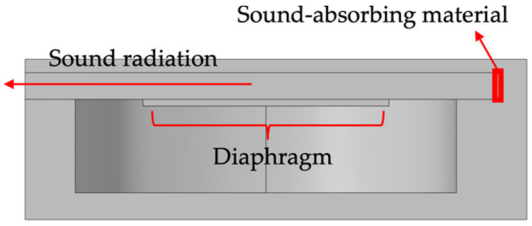

FIGURE 11. Cross-section of slim speaker system with sound-absorbing material.

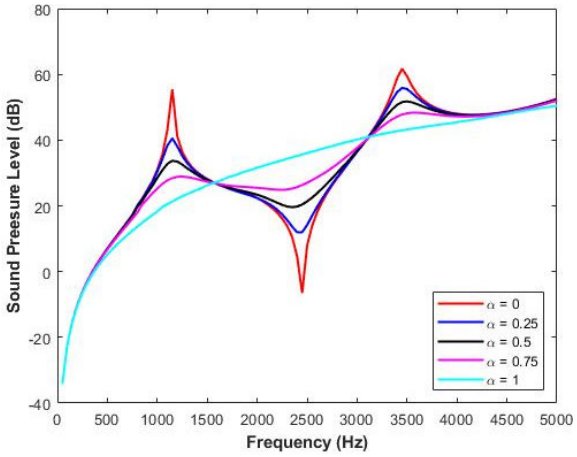

FIGURE 12. Sound pressure level of slim speaker system according to sound-absorption coefficient (α).

B. ENCLOSURE MODIFICATION

The frequency response of the speaker system is improved by modifying the enclosure shape. To reduce the dip effect caused by destructive interference, some in the industry empirically applied a slit at the top of the enclosure [22]. In this method, applying an additional sound-absorbing material is unnecessary, so the unit price increase can be prevented. Here, a slit of arbitrary size is applied, and the frequency response is calculated according to the slit position.

Figure 13 shows the frequency response according to the position of the 3mm wide slit on the top of the enclosure. The position of the slit is indicated at a distance from the point at which the sound is radiated, and numerical simulations are performed for three positions, respectively 10 mm, 35 mm, and 67.5 mm. When the slit position is 10 mm, there is no significant difference in frequency response compared to the existing model without the slit. When the slit position is 35 mm, the dip frequency shifts, but it can be confirmed that the sound pressure is slightly restored. When the slit position is 67.5 mm, it can be observed that the frequency response is significantly improved. Therefore, it can be observed that the frequency response improves as the slit position is closer to the reflective surface. It is possible to reduce the effect of destructive interference more effectively by placing the slit close to the reflective surface and translating the reflective waves into transmitted waves. However, if the slit size becomes huge, sound transmission performance

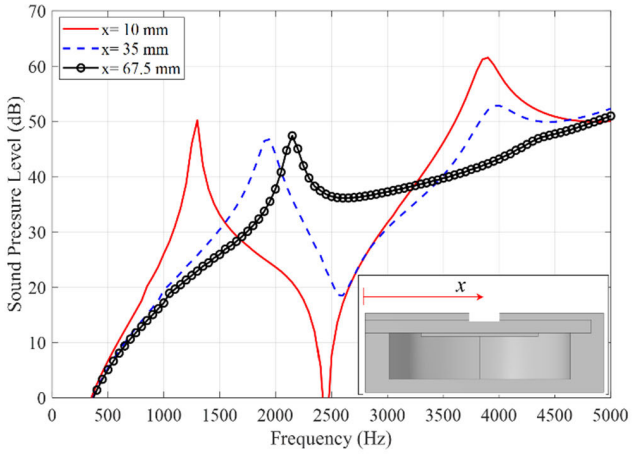

FIGURE 13. Sound pressure level of slim speaker system according to slit position.

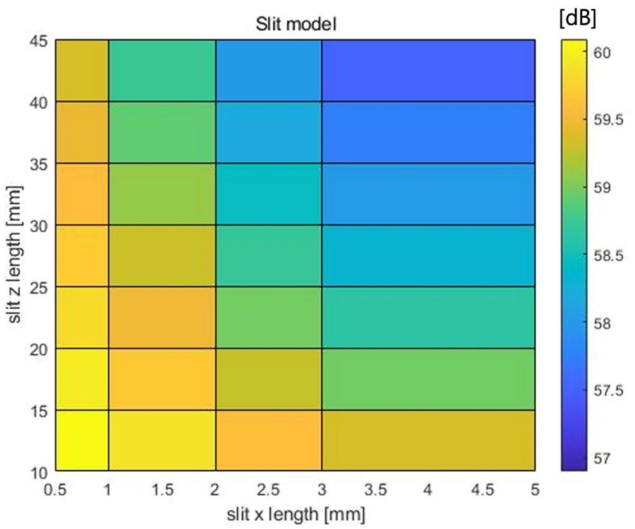

FIGURE 14. Amplitude of reflected sound pressure according to slit size.

at the corresponding location may deteriorate. Therefore, it is necessary to propose an appropriate slit size that minimizes sound pressure reduction.

The optimal slit size is now determined to achieve a better frequency response. A parametric study is conducted to determine the optimal slit size. The shape of the slit is a rectangle in consideration of the ease of mechanical processing, and the slit is located on the top of the enclosure so that the reflected wave can easily escape. The slit height and width are used as independent variables for the analysis. The sound pressure of the reflected wave is expressed as a dependent variable to be reduced. In order to express the sound pressure of the reflected wave, the measured sound pressure at two points separated by a distance s can be expressed using the following equations [14].

$$P_1(x) = P_i e^{-ikx} + P_r e^{-ikx} \tag{3}$$

$$P_2(x) = P_i e^{-ik(x+s)} + P_r e^{-ik(x+s)} \tag{4}$$

where P_i and P_r are the complex pressure amplitude of the incident and reflected waves, and k is the wave number. Combining Eqs. (3) and (4), P_i and P_r can be expressed for P_1 and P_2. Then, P_r can be defined as

$$P_r = \frac{-P_1 e^{-ik(x+s)} + P_2 e^{ikx}}{2isin(ks)} \tag{5}$$

The pressure amplitude of the corresponding reflected wave can be observed at the dip frequency by using the calculated sound pressure values at two points according to each condition. Figure 14 shows the amplitude distribution of the reflected wave when s is 2.5 mm and x is set to 57.5 mm. It can be seen that as the size of the slit increases, the effect of the reflected wave decreases. However, when the size of the slit increases, the sound is excessively radiated toward the slit, and the existing acoustic passage installed to induce the sound does not play a proper role. Therefore, to set the proper size of the slit, the amount of reduction in overall sound pressure level is observed. Table 5 shows the sound reduction of the overall sound pressure level and the sound pressure level around the dip frequency according to the size of the slit.

TABLE 5. Radiated sound reduction and sound pressure level at the dip frequency according to size of slit.

Slit size [mm]	Sound reduction [dB]	RMS around dip frequency range [dB, bandwidth = 400Hz]
1 × 10	0.02	26.3
1 × 30	0.96	28.9
1 × 50	2.81	36.0
3 × 10	0.39	27.6
3 × 30	1.96	34.4
3 × 50	4.86	43.4
5 × 10	0.59	28.1
5 × 30	2.52	37.6
5 × 50	5.73	47.6

It can be confirmed that as the size of the slit increases, the poor sound radiation around the dip frequency is improved, but the overall sound pressure level decreases. Therefore, a limiting condition is required for the sound reduction of the overall level to determine an appropriate slit size. Figure 15 shows each optimal size of the slit and associated sound pressure spectrum according to each minimum sound pressure reduction condition.

C. APPLYING IMPEDANCE MATCHED MEMBRANE

Reflected waves occur when the impedance is different at the boundary [23]. Therefore, the influence of the reflected wave can be eliminated by matching the impedances of different media. In order to match the characteristic impedance of air, impedance matching is conducted through a thin membrane. The enclosure's reflective wall is removed and replaced with a thin membrane. Simulations are performed by applying a membrane with arbitrary properties consistent with the

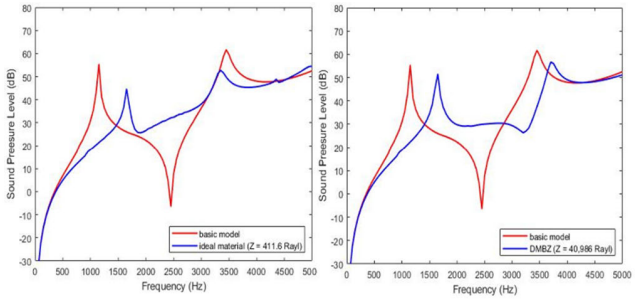

FIGURE 15. Comparison of numerical analysis results (a) when ideal material membrane is applied and (b) when DMBZ membrane is applied.

TABLE 6. Acoustic properties of membrane.

$65 \times 4 \times 0.8$ mm	Density [kg/m^3]	Acoustic speed [m/s]	Characteristics impedance [Rayl]
Ideal material	100	4.116	411.6
DMBZ	162	253	40986

characteristic impedance of air [24]. Figure 15(a) shows the numerical analysis results and compares the frequency response with the existing model. As expected, the frequency response is improved as the dip disappears. However, it is challenging to match the impedance of air with a general solid medium. Therefore, to solve this problem, metamaterials can be used to match the impedance of air [24]. However, applying the metamaterial of the type suggested by Park [24] is difficult due to the volume shortage problem of the slim-speaker system.

Therefore, in this paper, the effect of the reflected wave is reduced by applying a material with a lower characteristic impedance than a general solid material to the membrane. The analysis is performed by applying DMBZ material [25] to the membrane, and the material properties are shown in Table 6. Figure 15(b) shows the numerical analysis results. In the membrane model using DMBZ properties, it can be confirmed that the frequency response is improved as the influence of the reflected wave is reduced.

D. APPLYING MEMBRANE RESONATOR

A membrane resonator is a system that resonates at a specific frequency [26]. By matching the natural frequency of the resonant membrane to the deep frequency of about 2450Hz, it converts the acoustic energy of the incident wave into the vibration energy of the membrane in the frequency range to suppress the generation of reflected waves. Figure 16 shows the results of the natural frequency analysis by applying the material properties of the membrane having natural frequencies similar to the dip frequency. Table 7 shows the mechanical properties of the silicone membrane used in the analysis [27]. Figure 17 shows the numerical analysis results, and it can be seen that the frequency response improves in the dip frequency.

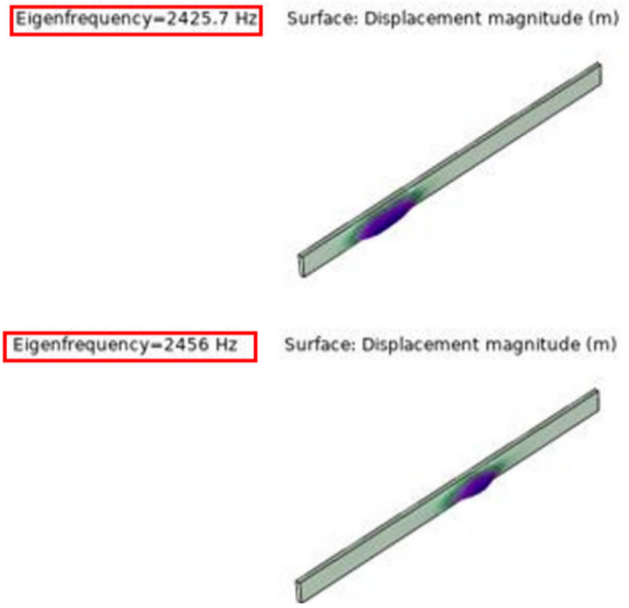

FIGURE 16. Modal analysis result of silicone membrane.

TABLE 7. Mechanical properties of silicone membrane.

Size [mm]	Density [kg/m^3]	Elastic module [Pa]	Poisson's ratio
$65 \times 4 \times 0.8$	980	1.9E6	0.48

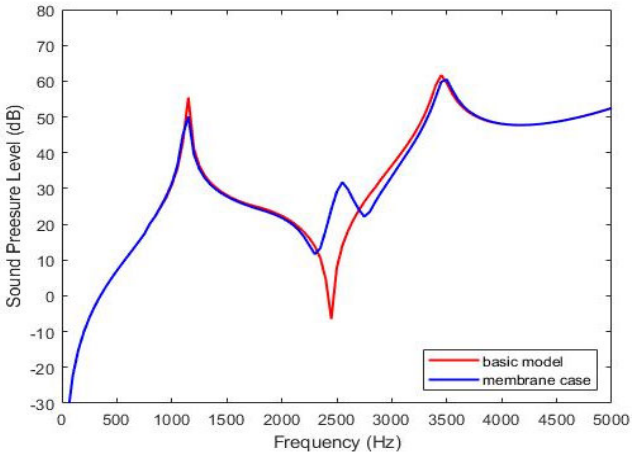

FIGURE 17. Numerical analysis results when resonant membrane is applied.

In addition, the active noise control method can be also applied to improve the frequency response at the dip frequency. However, complex acoustic resonance modes may occur in an internal space with a reflective surface, such as the inside of a slim speaker enclosure, making noise control difficult. To overcome these difficulties, it will be necessary to apply active noise control methods in environments with reflective surfaces.

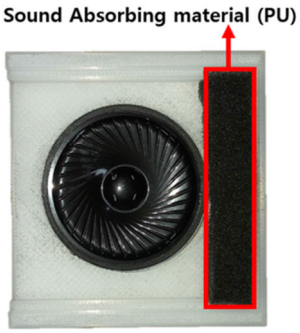

FIGURE 18. Experimental sample for test verification of sound-absorbing material application.

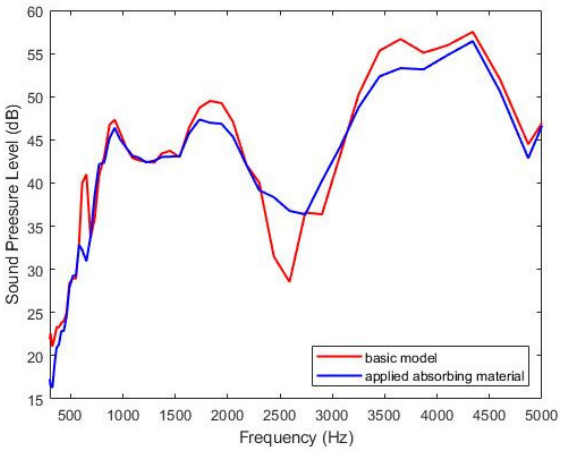

FIGURE 19. Experimental results of frequency response according to application of sound absorbing material.

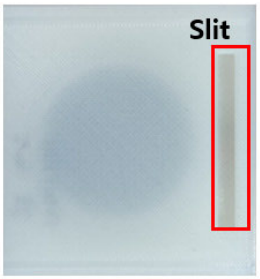

FIGURE 20. Experimental sample for test verification of slit application.

V. EXPERIMENTAL VALIDATION OF IMPROVED STRUCTURES

A speaker enclosure is manufactured using a 3D printer with PLA-i21 material, and the model is experimentally verified by comparing simulation and experimental results. However, for the membrane cases, it is not easy to make a membrane with the physical properties suggested in each case, so experimental verification is not conducted. Test verification is performed when the sound-absorbing material and the slit are applied.

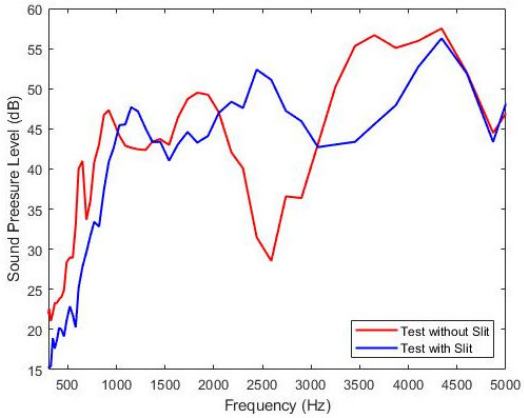

FIGURE 21. Experimental results of frequency response according to slit application.

A. APPLYING SOUND-ABSORBING MATERIAL

To verify the analysis results performed in Chapter 4, a sound-absorbing material made of PU (Polyurethane) is attached to the reflective surface, as shown in Figure 18. The test conditions are the same as the conditions described in Chapter 2. Figure 19 compares the frequency response when the sound-absorbing material is applied. The experimental results show a similar trend to the analytical results. Compared to the existing model, the SPL increased by about 12.2 dB at the dip frequency when the sound absorption material is applied.

B. ENCLOSURE MODIFICATION BY APPLYING SLIT

Figure 20 shows the shape of the enclosure produced by the 3D printer based on the results of Section IV-B. The sound test is performed under the same conditions as the test conditions described in Chapter 2. As shown in the experimental results of Figure 21, it can be seen that the frequency response is improved by making the slit, as the dip disappears as in the simulation result. When the slit is applied, the SPL at the dip frequency increases by about 23.8 dB compared to the existing model.

VI. CONCLUSION

In this paper, the sound radiation performance improvement of slim speakers in TVs has been studied. First, through the experiment, it is confirmed that the frequency response of the slim speaker system is poor at a specific frequency. Then, through numerical analysis, the cause of the poor frequency response at the dip frequency is investigated. It has been found that the radiated sound pressure is reduced due to the destructive interference caused by the 180-degree difference in the phases of the incident and reflected waves at the corresponding frequency. To improve sound radiation performance, installing a sound-absorbing material, a membrane on the inner reflective surface of the enclosure, and providing a slit at the top of the enclosure are proposed. Through experimental verification, in the case of installing sound-absorbing

material, it is shown that The SPL increased by about 12.2 dB at the dip frequency. In the case of the slit-applied enclosure, 23.8 dB is experimentally improved at the dip frequency. The improved speaker enclosure model presented in this study can be applied to TV and various multimedia applications.

ACKNOWLEDGMENT

The authors would like to thank Seungtaek Lee, Vice President of Geodsound, for his valuable advice and generous support on the speaker system, and also would like to thank to their mentor, Prof. Ki-Hyun Kim, who initially inspired them to start this study.

REFERENCES

[1] M. H. Lee, S. M. Seop, J. S. Kim, J. H. Hwang, H. J. Shin, S. K. Cho, K. W. Min, W. K. Kwak, S. I. Jung, C. S. Kim, and W. S. Choi, "Development of 31-inch full-HD AMOLED TV using LTPS-TFT and RGB FMM," *J. Soc. Inf. Display*, vol. 40, no. 1, pp. 802–804, Jul. 2012.

[2] P. Sun, J. Park, J. Kwon, and S. Hwang, "Development of slim speaker for use in flat TVs," *IEEE Trans. Magn.*, vol. 48, no. 11, pp. 4148–4151, Nov. 2012, doi: 10.1109/TMAG.2012.2197676.

[3] J.-H. Kwon, S.-M. Hwang, and K.-S. Kim, "Development of slim rectangular microspeaker used for minimultimedia phones," *IEEE Trans. Magn.*, vol. 43, no. 6, pp. 2704–2706, Jun. 2007, doi: 10.1109/TMAG.2007.893784.

[4] J. Kim, G. Lee, and J. Kim, "A computational model of vented band-pass enclosure using transmission line enclosure modeling," in *Proc. 131th Conv. Audio Eng. Soc.*, New York, NY, USA, Oct. 2011, p. 8499.

[5] H. Takewa, S. Saiki, S. Kano, and A. Inaba, "Slim-type speaker for flat-panel televisions," *IEEE Trans. Consum. Electron.*, vol. 52, no. 1, pp. 189–195, Feb. 2006, doi: 10.1109/TCE.2006.1605046.

[6] M. R. Bai and J. Liao, "Acoustic analysis and design of miniature loudspeakers for mobile phones," *J. Audio Eng. Soc.*, vol. 53, no. 11, pp. 1061–1076, Nov. 2005.

[7] K. Minami and Y. Kajikawa, "A study on frequency response analysis of micro-speaker using equivalent circuit and finite element method," in *Proc. IEEE 9th Global Conf. Consum. Electron. (GCCE)*, Kobe, Japan, Oct. 2020, pp. 723–725, doi: 10.1109/GCCE50665.2020.9292039.

[8] D.-C. Kim and H.-Y. Jeong, "An optimal design of the internal space in a micro-speaker module," *Int. J. Precis. Eng. Manuf.*, vol. 16, no. 6, pp. 1141–1147, Jun. 2015, doi: 10.1007/s12541-015-0148-4.

[9] S. Oh, "Speaker classification," in *Theory and Design of Loudspeaker*. South Korea: SeokHakDang, 2011.

[10] V. M. Garcia-Alcaide, S. Palleja-Cabre, R. Castilla, P. J. Gamez-Montero, J. Romeu, T. Pamies, J. Amate, and N. Milan, "Numerical study of the aerodynamics of sound sources in a bass-reflex port," *Eng. Appl. Comput. Fluid Mech.*, vol. 11, no. 1, pp. 210–224, Jan. 2017, doi: 10.1080/19942060.2016.1277166.

[11] J. Backman, "The nonlinear behavior of reflex ports," in *Proc. 98th Conv. Audio Eng. Soc.*, Espoo, Finland, Feb. 1995, p. 3999.

[12] Y.-W. Jiang, D.-P. Xu, Z.-X. Jiang, J.-H. Kim, K.-H. Park, and S.-M. Hwang, "Analysis and application of screens for acoustic impedance in a speaker box with a passive radiator to decrease standing-wave influence," *Appl. Sci.*, vol. 10, no. 3, p. 866, Jan. 2020, doi: 10.3390/app10030866.

[13] S. Lee, K. Park, S. Park, J. Lee, and H. Park, "Improved sound quality by using the exciter speaker in OLED panel," *J. Soc. Inf. Display*, vol. 28, no. 3, pp. 297–307, Nov. 2019, doi: 10.1002/jsid.855.

[14] F. Fahy and C. Schofield, "A note on the interaction between a Helmholtz resonator and an acoustic mode of an enclosure," *J. Sound Vibrat.*, vol. 72, no. 3, pp. 365–378, Oct. 1980, doi: 10.1016/0022-460X(80)90383-1.

[15] D. Li and L. Cheng, "Acoustically coupled model of an enclosure and a Helmholtz resonator array," *J. Sound Vibrat.*, vol. 305, nos. 1–2, pp. 272–288, Aug. 2007, doi: 10.1016/j.jsv.2007.04.009.

[16] S.-H. Park and S.-H. Seo, "Low-frequency noise reduction in an enclosure by using a Helmholtz resonator array," *Korean Soc. Noise Vibrat. Eng.*, vol. 22, no. 8, pp. 757–762, Aug. 2012, doi: 10.5050/KSNVE.2012.22.8.756.

[17] I. Demirel, "Analysis of loudspeaker's placement angle and direction on frequency response and sound pressure level in TV applications," *Arch. Acoust.*, vol. 46, no. 1, pp. 79–85, 2021, doi: 10.24425/aoa.2021.136562.

[18] Y.-J. Ji and S.-C. Jung, "Slim enclosure speaker with side acoustic emission structure," U.S. Patent 2014 0 301 587 A1, Mar. 31, 2014.

[19] M. J. Lucs, R. Noreeen, L. D. Sutherland, J. Cole III and M. Junger, "The acoustic characteristics of turbomachinery cavitiess," NASA Marshall Space Flight Center, Alabama, USA, NASA Rep. 4671, 1995. [Online]. Available: https://ntrs.nasa.gov/citations/19950022299

[20] L. Kinsler, A. Frey, A. Coppens, and J. Sanders, "Pipes, resonators, and filters," *Fundamentals of Acoustics*, 4th ed. Hoboken, NJ, USA: Wiley, 2000.

[21] P. D'Antonio and T. J. Cox, "Room optimizer: A computer program to optimize the placement of listener, loudspeakers, acoustical surface treatment and room dimensions in critical listening rooms,"in *Proc. 103rd Conv. Audio Eng. Society*, New York, NY, USA, Sep. 1997, p. 4555.

[22] H. Lee, J.-H. Han, H. Kim, and K. Kim, "Improved sound pressure characteristics of slim speaker," in *Proc. Korea Soc. Noise Vib. Eng. Spring Conf.*, Je-ju, South Korea, Apr. 2018, p. 232.

[23] S. Kim, "Acoustic impedance termination," M.S. thesis, Dept. Mech. Eng., Yonsei Univ., Seoul, South Korea, 2012.

[24] C. M. Park and S. H. Lee, "Zero-reflection acoustic metamaterial with a negative refractive index," *Sci. Rep.*, vol. 9, no. 1, p. 3372, Mar. 2019.

[25] A. J. Swank, O. S. Sands, and M. A. B. Meador, "Polyimide aerogels and porous membranes for ultrasonic impedance matching to air," Glenn Res. Center, Cleveland, OH, USA, Tech. Rep. NASA/TM-2014-218400, Oct. 2014.

[26] Y. Li, I. Oh, J. Chen, and Y. Hu, "A new design of dielectric elastomer membrane resonator with tunable resonant frequencies and mode shapes," *Smart Mater. Struct.*, vol. 27, no. 6, Jun. 2018, Art. no. 065029, doi: 10.1088/1361-665X/aab996.

[27] C. Gao, D. Halim, and X. Yi, "Study of bandgap property of a bilayer membrane-type metamaterial applied on a thin plate," *Int. J. Mech. Sci.*, vol. 184, Oct. 2020, Art. no. 105708, doi: 10.1016/j.ijmecsci.2020.105708.

JOON-YEON PARK received the B.S. and M.S. degrees from the Department of Mechanical Engineering, Tech University of Korea, Siheung, South Korea, in 2020 and 2022, respectively. He is currently an Acoustics Researcher with LIG Nex1. His research interests include acoustic-structural coupled finite element analysis and acoustic testing.

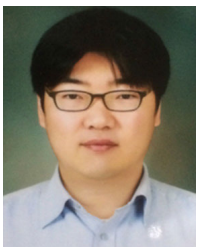

JE-HEON HAN (Member, IEEE) received the Ph.D. degree in mechanical engineering from Texas A&M University, in 2013. He was with the Hyundai-Kia Research and Development Center and Korea Aerospace Research Institute as a NVH Development Engineer and a Senior Engineer, respectively. Currently, he is an Associate Professor with the Department of Mechanical Engineering, Tech University of Korea. His research interests include vibration analysis, array signal processing, and the non-destructive evaluation of mechanical systems.